Globotriaosylceramide-Related Biomarkers of Fabry Disease Identified in Plasma by High-Performance Thin-Layer Chromatography - Densitometry- Mass Spectrometry

> (i) The corrections made in this section will be reviewed and approved by a journal production editor.

Carmen Jarne[a], Luis Membrado[a], María Savirón[b], Jesús Vela[c], Jesús Orduna[b], Rosa Garriga[d], Javier Galbán[c], Vicente L. Cebolla[a],* vcebolla@icb.csic.es

[a]Instituto de Carboquímica, CSIC, C/ Miguel Luesma, 4, 50018 Zaragoza, Spain

[b]CEQMA-CSIC, Facultad de Ciencias, Universidad de Zaragoza, 50009 Zaragoza, Spain

[c]Departamento de Química Analítica, Universidad de Zaragoza, 50009 Zaragoza, Spain

[d]Departamento de Química Orgánica y Química-Física, Universidad de Zaragoza, 50009 Spain

*Corresponding author: Vicente Luis Cebolla Burillo, Instituto de Carboquímica, ICB-CSIC C/ Miguel Luesma, 4, 50018 Zaragoza, Spain

Abstract

Identification of 19 molecular species of globotriaosylceramides (Gb_3) in extracts from a Fabry's plasma patient and a healthy control was performed by High-Performance Thin-Layer Chromatography (HPTLC)-densitometry and online coupling to Mass Spectrometry (MS).Separation was carried out on LiChrospher plates using Automated Multiple Development (AMD). Densitometry was performed on twin plates by combining detection in the visible at 550 nm, through previous on-plate orcinol derivatization, and by Ultraviolet 190 nm, using a non-impregnated plate. The latter was directly coupled to an ion-trap mass spectrometer through an automated elution-based interface.Gb_3 molecular species, which were identified by HPTLC- Electrospray Mass Spectrometry (+)-MS and confirmed by MS/MS or HPTLC-Atmospheric Pressure Chemical Ionization Mass Spectrometry (+)-MS, are: five isoforms of saturated Gb_3; seven isoforms of methylated Gb_3; and seven species with two additional double bonds. Twelve of these species were previously reported as biomarkers of Fabry's lysosomal disorder using a Liquid Chromatography-MS-based method, and the other seven are structurally similar, closely related to them.Saturated Gb_3 isoforms migrated on LiChrospher plate in one of the separated peaks corresponding to the migration zone of ceramide trihexosides standard. Instead, methylated and unsaturated Gb_3 species co-migrated with sphingomyelin species.Ion intensity ESI-MS profiles show that saturated Gb_3 species in Fabry's plasma were in higher concentration than in control sample.Before applying the Thin-Layer Chromatography (TLC)-MS interface on HPTLC separated peaks, its positioning precision was first studied using ceramide tri-hexosides as model compound. This provided information on Gb_3 peak broadening and splitting during its migration.

Keywords: HPTLC; HPTLC-ESI-MS; HPTLC-APCI-MS; AMD; orcinol derivatization; Scanning densitometry; Sphingolipids; globotriaosylceramide; Fabry's disease

1 Introduction

Fabry disease is an X-linked lysosomal storage disorder caused by a deficiency of the enzyme α-galactosidase A, which results in the progressive accumulation of Gb_3, globotriaosylsphingosine (Lyso-Gb_3), and digalactosylceramide (Gal-Gal-Cer) in lysosomes [1,2]. Detection of these glycosphingolipid (GSL) metabolites in urine and plasma are the

standard diagnostic for this disorder which involves renal failure, cardiovascular disease and other complications associated with reduced quality of life and early mortality [3,4].

A number of Gb_3-related molecular species in plasma and urine from Fabry patients were detected which make up a metabolic profile that may provide insight into the pathophysiology of Fabry disease, and in understanding the underlying biochemical mechanisms involved. Thus, twenty-four molecular species related to Gb_3 were considered as biomarkers of Fabry disease using a multivariate statistical analysis based on data from reversed phase-Liquid Chromatography (LC) coupled to tandem Mass Spectrometry (MS) [5,6]. Identified molecular species were mostly methylated-Gb_3 and unsaturated species. LC-MS-based metabolomics has proven to be an important tool for searching and identifying biomarkers due its high sensitivity, specificity, and robustness. Instead, High-Performance Thin-Layer Chromatography (HPTLC), together with densitometry, is a popular technique used in combination with other techniques of biochemistry and molecular biology, mostly for the separation of lipids in classes although is not usually considered as adequate for a detailed characterization of a complex sample of lipids. However, its direct coupling with MS has made a strong progress over the past decade, so that HPTLC separation of sample into lipid-classes, detection by densitometry and MS coupling currently provide a simple but rapid and powerful approach for the structural identification of lipids present in biological extracts, from the selected bands separated on the chromatographic plate, allowing their exact identification by their *m/z*, and confirmation by their collision-induced dissociation MS/MS data or other techniques.

Densitometry is the core of detection and centerpiece for coupling HPTLC and MS. For sphingolipid (SL) analysis, derivatization using orcinol [7,8], charring with copper sulfate-phosphoric acid reagent [16], impregnation with primuline [8,10-13,15], and immunostaining [8,14], were reported in the literature as an intermediate step before MS. Several plates in parallel were frequently used. For direct coupling, an underivatized twin plate has usually been employed under the same chromatographic conditions [9]. Primuline-impregnated plates were also demonstrated to be compatible with MS analysis [10,12,15].

HPTLC-densitometry has mostly been coupled either with desorption techniques such as Matrix-Assisted Laser Desorption/ionization (MALDI), Desorption Electrospray Ionization (DESI), or by another approach consisting of Electrospray Ionization (ESI) or Atmospheric Pressure Chemical Ionization (APCI) via on-plate automated extraction using a dedicated interface. Overall, HPTLC separation provided a reduction in complexities, both of the sample and of the resulting mass spectra, which allowed for complete identification of lipid species in lipidomic mixtures. For SL analysis, HPTLC-densitometry-DESI-MS, MS/MS allowed detection of 30 species from 11 classes of SL in human lens, including minor GSL, and novel ether-linked phosphatidic acid species. Likewise, LacCer with a sphinganine backbone were exclusively observed using this technique [10]. These compounds, effectively identified by HPTLC-MS, were not identified by direct-infusion MS of the lipid extracts due to ion suppression effects. Moreover, complex gangliosides (GQ1, GT1, GD1, GM1), and GD1a and GD1b isomers were directly identified from tissue slices of rat brain by HPTLC-densitometry-DESI-MS, MS/MS even if separation was only partially resolved [7]. All this was accomplished despite the limited resolution of DESI experiments, as lipids can only be separated over a short distance because the DESI source had a maximum mobile distance of 35.8 mm.

MALDI has been the most widely used MS ionization technique coupled to HPTLC. Frequently combined with TOF, MALDI-MS, MS/MS was mostly used to profile SL and GSL, identify their molecular species, or to image their distribution on the plates, from monocytic THP-1 cells [16]; from mouse kidney, spleen, and small intestine [8]; from skeletal mice muscle, brain mice tissue, human serum, and murine myoblasts [11]; and for differentiating human bone marrow mesenchymal stem cells toward osteoblasts [14]. The difficulty in obtaining quantitative information due to the current configuration of MALDI equipment was reported [17,18]. Likewise, a careful selection of matrix is crucial to overcome ions suppression effects [19].

Another possibility that is being explored for HPTLC-MS coupling is the use of an elution-based interface which allows to locate the desired band on the dry plate, after sample separation and solvent removal, automatically extract it using an appropriate solvent, and transfer it to any MS equipment. In this way, molecular species of SM and some saturated Gb_3 species in plasma extracts were directly identified from their respective lipid-classes, separated by Automated Multiple Development (AMD) on silica gel HPTLC plates [12,15]. The interface was coupled either to a combination of ESI^+ and $APCI^+$-MS [15], or to tandem MS, using ESI^+-MS/MS [12]. Likewise, ten Ceramide subclasses, including different sphingoid bases and fatty acyl chains, were separated on LiChrosper HPTLC silica gel plates by AMD, and characterized by ESI^--MS, MS/MS [9].

The interface has several aspects that make it interesting for sphingolipid, and in general, lipid analysis: its potential connection to any MS instrument opens up a range of analytical possibilities; its speed of access to the extraction of the desired bands on the plate; and the precision of the extraction, an aspect that has not been studied in depth, and that has been considered in our work. Moreover, its use is suitable for the analysis of glycosphingolipids since sialic acids are not lost when using the interface, unlike the case of MALDI, where this happens due to the acidity of the matrices used. [13,20].

The aim of this work was to evaluate whether an HPTLC-densitometry-MS approach using the automated elution-based interface is adequate for identifying Gb_3-related Fabry's biomarkers in human plasma. This study has mostly used HPTLC-ESI(+)-MS focusing on Gb_3-related molecular species with m/z between 1000 and 1200 Da. HPTLC-ESI$^+$-MS/MS or HPTLC-APCI$^+$-MS have also been used for ion identity confirmation.

The positioning accuracy of the interface was first studied from a ceramide tri-hexosides standard as model compound, and then applied to the separate peaks of sample on the chromatographic plate. This provided information on the reasons why the Gb_3 peak experiences widening and even splitting during its migration under the studied chromatographic conditions.

Extracts of plasma from a Fabry's patient and healthy control were studied. Interesting information on samples was obtained from densitometry at Vis 550 nm through orcinol derivatization. Its combined use with a twin, non-impregnated plate (UV 190 nm) for MS coupling was useful for obtaining information through densitometry.

2 Experimental

2.1 Standards, samples and chemicals

Sphingomyelin, SM [$\geq$97%; (85187-10-6) CAS], ceramide tri-hexosides [Gb_3, >98+%; (71965-57-6) CAS], lyso-ceramide trihexosides, lyso-Gb_3 [>98% (126550-86-5) CAS], lactosyl ceramide, LacCer [$\geq$98%, (4682-48-8) CAS], glucosyl ceramide, GlcCer [$\geq$98%, (9884) CAS] were obtained from Matreya, LLC (State College, PA). Fatty acyl composition of standards can be found elsewhere [21].

Plasma samples were obtained from the Institute of Health Sciences (Zaragoza, Spain) after approval of the Ethical Committee of Aragon (CEICA, Spain). Informed consent was obtained from the human subjects. Fabry's sample comes from a patient undergoing a month of enzyme replacement therapy.

Methanol (MeOH, HPLC-grade, 99.9%) and dichloromethane (DCM, HPLC-grade, 99.5%) were purchased from Scharlau (Barcelona, Spain). Chloroform ($CHCl_3$, HPLC-grade, 99.0%) and sodium hydroxide (American Chemical Society grade, 98.0%), were purchased from Panreac (Barcelona, Spain). Orcinol [(6153-39-5) CAS] was purchased from Sigma-Aldrich (Madrid, Spain).

LiChrospher plates (20 × 10 cm) from Merck (Darmstadt, Germany) were employed. They were pre-washed with methanol and kept in dessicator in N_2 atmosphere.

2.2 Sample treatment

Neutral SL extracts were obtained from plasma using a standard sample preparation procedure which involves centrifugation, alkaline hydrolysis and extraction, as was described elsewhere [12,15]. Thus, for 250 μL plasma aliquots, vials were extracted (30 min with 2 mL of DCM–MeOH, 1:1, v/v) in a shaker, and centrifuged for 10 min at 5000 rpm. Precipitated protein was removed. The upper layer was subjected to alkaline hydrolysis by adding 75 μL of 2 M sodium hydroxide, and incubated with magnetic stirring (2 h at 40℃). Subsequently, 1 mL of H_2O and 1 mL of MeOH were added, and vials were centrifuged at 5000 rpm for 20 min. The lower layer containing the neutral sphingolipids was then transferred to a vial and dried under N_2. Samples were reconstituted in 250 μL of DCM–MeOH,1:1, v/v for HPTLC analysis.

2.3 HPTLC-densitometry

All the equipment employed for sample application, chromatographic development, and densitometry is from CAMAG (Muttenz, Switzerland).

Sample and standard solutions were applied as 4-mm bands on the corresponding plate by using the Automatic TLC Sampler (ATS4) system.

Solutions of standards (lyso-Gb_3, Gb_3, LacCer, GlcCer; concentration: 0.1 μg/μl per standard in DCM:MeOH, 1:1 v/v; application volume: 0.1-10 μl/band; applied effective mass: 0.01-1 μg/band) were applied, either individually or as a mixture, for monitoring migration distance (m.d.) after chromatography.

A variable number of plasma sample extracts dissolved in DCM:MeOH (1:1) (25-30 μL/band) and standard solutions (solution concentration: 0.1 μg/μl in DCM:MeOH (1:1), injection volume: 0.1-10 μL/band, injected mass: 0.01-1 μg/band) were applied on the same plate. Each of the plasma samples and standards were injected in triplicate. The distance between tracks was 10.6 mm; distances from the lateral and lower plate edges were 10 mm. One or more tracks were left empty, as blanks. Chromatographic development was performed using the Automated Multiple Development (AMD2) system under the conditions detailed in Table 1.

alt-text: Table 1-

AMD conditions used for standards and plasma extract HPTLC development

DCM(Vol. %)	MeOH(Vol. %)	Migration distance(mm)
0	100	20
60	40	30
60	40	30
60	40	30
60	40	30
60	40	30
70	30	50
80	20	60
90	10	90

After separation, two procedures were used for detection. Orcinol derivatization was carried out as follows: the plate was submitted to post-impregnation using 0.2 g of orcinol in 100 mL of 10% H_2SO_4 using the CAMAG Impregnation Chamber during 2 s. The impregnated plate was heated during 15 min at 100°C using the CAMAG Plate Heater 3. Densitometric detection was then performed at Vis 550 nm.

UV densitometry at 190 nm was done from a non-impregnated plate, which was used for MS coupling through the interface.

2.4 Thin Layer Chromatography-Mass Spectrometry (TLC-MS) interface

Non-impregnated plates were utilized for MS coupling through the interface. Bands were eluted online into an ion trap MS (Esquire 3000 Plus system, Bruker Daltonics, Bremen, Germany) with ESI and APCI sources, by using the TLC-MS interface 2 (CAMAG), equipped with an oval, 4 × 2-mm extraction head under the conditions described elsewhere [17,18]. MeOH was delivered at 0.2 mL/min by using a PU-2080 HPLC pump (Jasco, Tokyo, Japan). The eluate is directed through a 2-μm stainless steel frit to remove silica gel and then directed into the MS via the outlet capillary. The operating scheme of the interface was described elsewhere [18]. Working steps are: bypass, first band extraction, air cleaning and second band extraction ~~are idealized in the Graphical Abstract of this work~~. Blanks of silica gel were extracted as control, depending on the case.

ESI-MS was conducted in positive mode, with capillary and endplate offset voltages of 4000 and −500 V, nebulizer pressure 40 psi; flow and temperature of drying gas 9 mL/min and 350°C, respectively. Spectra were acquired in the m/z 300–1500 range at the standard/normal scan mode. APCI ionization conditions were as follows: capillary voltage 2000–3000 V; current intensity 4500 nA; nebulizer pressure 45 psi; flow and temperature of drying gas 5 mL/min and 350°C, respectively; vaporization temperature 450°C. Full scans were recorded up to m/z 1500 in positive ion mode.

2.5 Experiments on precision of TLC-MS interface positioning

They were carried out exclusively on three aliquots (T1, T2 and T3) of a Gb_3 standard solution (1 μg/μl in DCM:MeOH, 1/1, v/v), which were applied 10.6 mm apart as 4-mm bands on a non-impregnated LiChrospher plate, and were developed using the AMD conditions specified in Table 1.

From UV densitometry coordinates, the 2 × 4 mm-oval extraction head was positioned on the center of the T1 band (x=0), and a 2-mm zone (counting from the center) was automatically extracted and sent to MS via the interface. Thus, the HPTLC-ESI$^+$-MS spectrum of the central part of Gb_3 standard band is shown in Figure 1A.

alt-text: Figure 1-

Figure 1.-
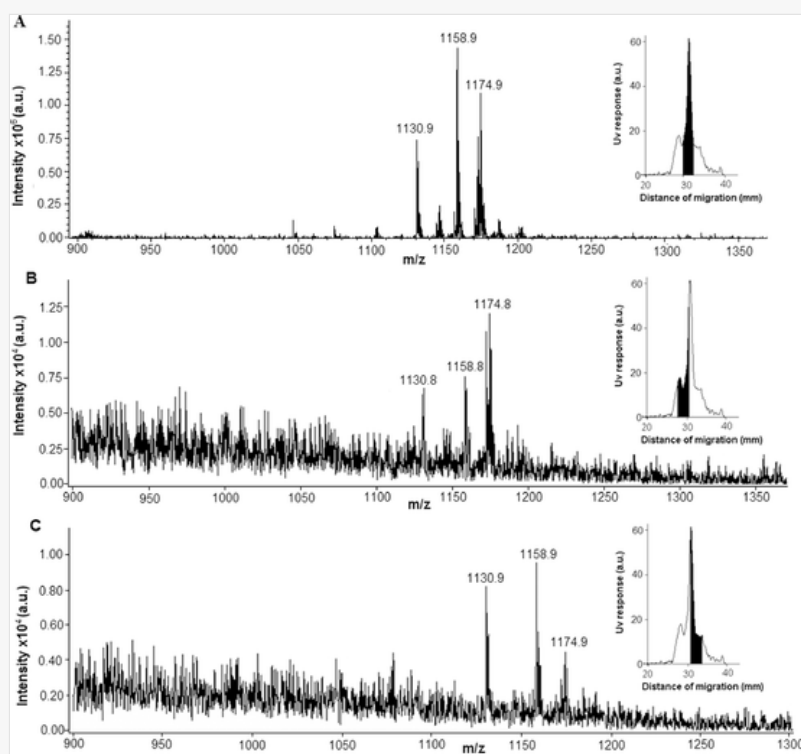
A) HPTLC-ESI$^+$-MS spectrum of ceramide tri-hexosides standard, applied as a 4-mm band and developed 30 mm using AMD2 on a LiChrospher plate. To obtain the spectrum, the interface head was positioned in the center of the band (x=0). **B)** HPTLC-ESI$^+$-MS spectrum of the first half of the band (center in x=-1 mm). **C)** HPTLC-ESI$^+$-MS spectrum of the second half of the band (center in x=+1 mm). Ions at m/z 1175, 1159 and 1131 are, respectively, sodium adducts of Gb$_3$ d18:1;C24:0 2-OH, Gb$_3$ d18:1;C24:0 and Gb$_3$ d18:1;C22:0. See text for interpretation.

After this, the oval extraction head was precisely positioned on the left part of the T2 band (x=-1 mm). In this way, the corresponding plate zone punched out by the head consists of a mixture of silica gel and standard. Silica gel was filtered in the interface, and the eluate was extracted online and sent to the mass spectrometer to obtain the HPTLC-ESI$^+$-MS spectrum of the left part of the Gb$_3$ band (Figure 1B).

Later, this way of proceeding was repeated by positioning the extraction head on the right part of the T3 band (x=+1 mm) to obtain the HPTLC-ESI$^+$-MS spectrum of the right part of the Gb$_3$ band (Figure 1C).

3 Results and discussion

3.1 Composition of ceramide tri-hexosides (Gb3) standard and interface positioning

Standards of biomolecules are complex mixtures in themselves although less than real biological samples. They allow methods to be validated with verifiable results.

Before analyzing Gb$_3$ biomarkers in plasma, we here tested the performance of the interface for confirming, by HPTLC-densitometry-MS, the fatty acyl composition of a ceramide tri-hexosides standard (Gb$_3$). Likewise, the positioning of the interface was tested to evaluate its precision in order to obtain mass spectra of different zones of the standard chromatographic band, which should allow to obtain the distribution of the different fatty-acyl subclasses in function of the migration distance within the chromatographic Gb$_3$ peak. This study has also allowed us to establish the conditions of interface application for the characterization of unresolved peaks in the corresponding plasma samples.

Regardless of detection system used, Gb$_3$ standard usually provides a wide or multiple peak which probably shows co-migration of different sub-classes of molecular species. This phenomenon was reported in the literature [13,16,22,23].
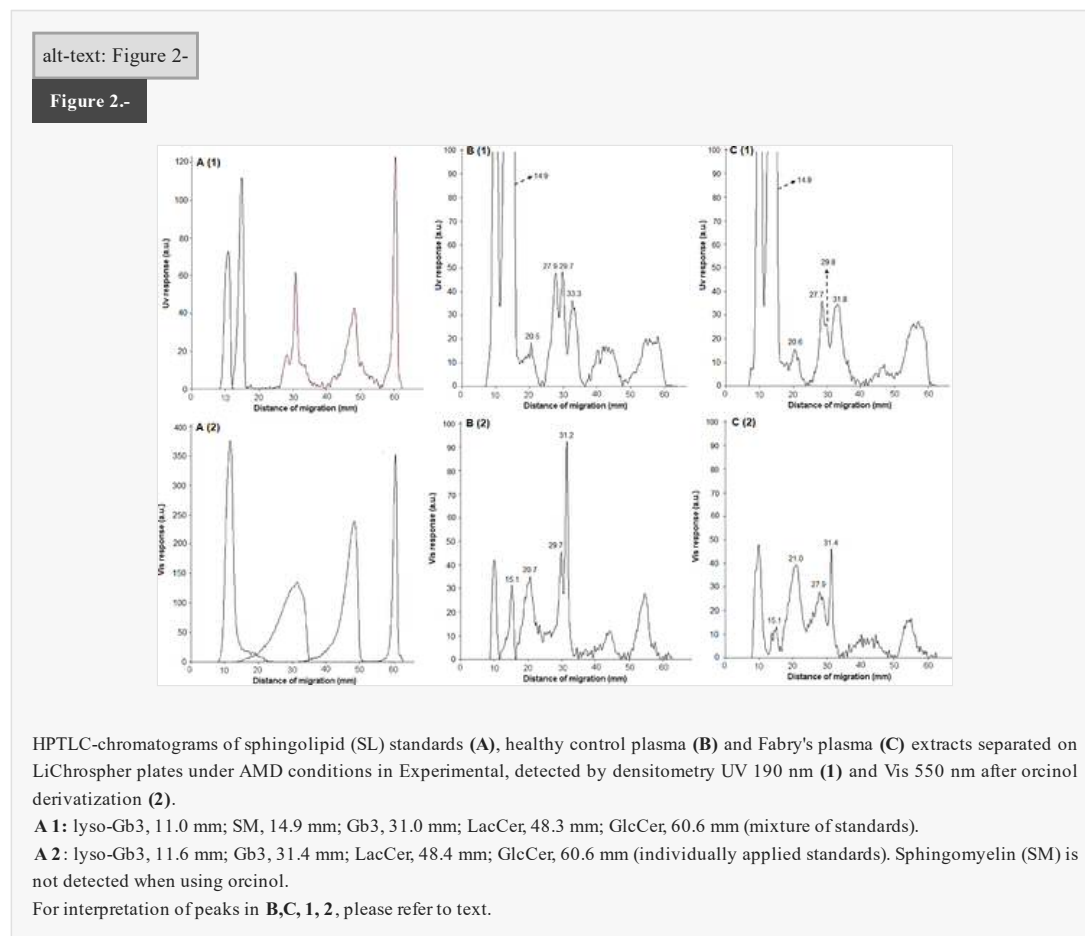
As explained in Experimental (section 2.5), the HPTLC-ESI$^+$-MS spectra of the central, left, and right parts of Gb$_3$ standard band were obtained from T1, T2 and T3 solution aliquots, and are shown in Figures 1A, 1B and 1C, respectively.

The zones punched out by the interface can be seen in the corresponding box shown in the Figure 1. In the cases of the left and right parts, the corresponding plate zone punched out by the head consists of a mixture of silica gel and standard. Silica gel was filtered in the interface, and the eluate was extracted online and sent to the mass spectrometer. Thus, in these cases, the corresponding plate zone punched contain lower concentration in Gb$_3$ that in the case of the central part of Gb$_3$ standard (x=0). For this reason, intensity and S/N ratio of the corresponding spectra are lower.

Ceramide tri-hexosides standard consists of Gb$_3$ isoforms with a distribution of different fatty acyl substitutions. ESI-MS spectrum of the whole standard band shows the following ions, as sodium adducts. The most abundant Gb$_3$-related

structures are: *m/z* 1158.9 (d18;C24:0), *m/z* 1174.9 (d18;C24:0 2-OH), and *m/z* 1130.9 (d18;C22:0). Other less-abundant sodium adducts found were: d18;C16:0 (*m/z* 1046.9), d18;C18:0 (*m/z* 1074.9), d18;C20:0 (*m/z* 1103.9), and d18;C22:0 2-OH (*m/z* 1146.9). The spectrum obtained by HPTLC-MS shows the complexity of standard composition, and is in agreement with the fatty acyl composition provided by the manufacturer, which specifies a percentage of 29% (d18;C24:0), 19% (d18;C24:0 2-OH), and 17% (d18;C22:0), for the three most abundant species, respectively [21].

The HPTLC-ESI$^+$-MS spectrum of the left part (x=-1 mm) of Gb$_3$ peak shows, as the preponderant ion, the sodium adducts of d18;C24:0 2-OH (*m/z* 1174.8), with d18;C24:0 (*m/z* 1158.8) and d18;C22:0 (*m/z* 1130.8) as minority species. Therefore, results suggest that d18;C24:0 2-OH, with a hydroxy-fatty acyl is concentrated in the left part of the peak. Instead, saturated d18;C24:0 (*m/z* 1158.9) and d18;C22:0 (*m/z* 1130.9) are majority species in the right part (x=+1 mm) of the peak. This is consistent with the coexistence of Gb$_3$ subclasses, where more polar hydroxyl-fatty acyls are more retained species (lower migration distance) on silica gel with regard to the Gb$_3$ with saturated/mono-unsaturated fatty acyls which are less retained, having a slightly higher migration distance. This explains Gb$_3$ splitting (Figure 1) or broadening (in Figure 2A). Likewise, it should also be considered that Gb$_3$ isoforms with different types of hexose, either glucose or galactose, may also coexist in the peak. They would have a very similar migration distance and would be indistinguishable by MS.

HPTLC-chromatograms of sphingolipid (SL) standards **(A)**, healthy control plasma **(B)** and Fabry's plasma **(C)** extracts separated on LiChrospher plates under AMD conditions in Experimental, detected by densitometry UV 190 nm **(1)** and Vis 550 nm after orcinol derivatization **(2)**.
A 1: lyso-Gb3, 11.0 mm; SM, 14.9 mm; Gb3, 31.0 mm; LacCer, 48.3 mm; GlcCer, 60.6 mm (mixture of standards).
A 2: lyso-Gb3, 11.6 mm; Gb3, 31.4 mm; LacCer, 48.4 mm; GlcCer, 60.6 mm (individually applied standards). Sphingomyelin (SM) is not detected when using orcinol.
For interpretation of peaks in **B,C, 1, 2**, please refer to text.

Another conclusion of this preliminary study is that the positioning of the interface allows to carry out a precise and adequate MS characterization of the bands, and even of zones within a band, separated by HPTLC.

3.2 HPTLC separation and densitometric detection of plasma samples

Figure 2 shows the HPTLC-densitograms of individual standards (A) and plasma samples, healthy control (B) and Fabry's plasma (C), separated on LiChrospher plates and developed using AMD. Detection was performed using UV at 190 nm (1), and Vis at 550 nm after orcinol treatment (2), according to experimental section. Migration of standards takes place according the polarity and number of carbohydrate units of sphingolipid.

Although only unsaturated lipids are detected by densitometry at 190 nm, this works as a general detection mode for sphingolipids, as sphingosine moiety in their respective ceramides has a double bond.

Derivatization with orcinol is selective for detecting glycosphingolipids (lyso-Gb$_3$, Gb$_3$, LacCer and GlcCer standards), and is based on dehydration of sugar to furfural, and its reaction with orcinol in sulfuric medium to produce a colored condensation complex [Instruction: 26-28 should be changed to new references 24-26, as old references 24 and 25 have been deleted][7,26-28]. As can be seen in Figure 2A, SM standard had not response in orcinol derivatization. This was useful for checking the presence of glycosphingolipids in each separated plasma band. These conditions were useful for checking whether HPTLC separated peaks contained some of the Gb$_3$-biomarker species.

Densitograms of Fabry's and control plasma samples obtained under the above conditions show an intense peak in UV 190 nm at migration distance (m.d.) of 14.2 and 14.9 mm, respectively) migrating at a similar m.d. that SM standard. This peak mostly corresponded to SM species under these conditions, as it will be detailed below. However, this peak shows a residual signal at 550 nm after treatment with orcinol. Therefore, it seems that low concentrated-GSL species are co-eluting together with SM species.

In the migration area between 20 and 34 mm, both samples (Fabry and control) show similar chromatographic profiles with slight differences in migration distances. Four peaks are detected by UV and only three are visualized with orcinol. UV peaks were at 20.5, 27.9, 29.7 and 33.3 mm for control sample; and 20.6, 27.7, 29.8 and 31.8 mm for Fabry's sample. In orcinol, the following peaks are visualized in that zone: 20.7, 29.7 and 31.2 for control; and 21, 27.9 and 31.4 for Fabry's sample.

Selection of peaks for transferring to ESI or APCI-MS, via the elution-based interface, was done from a non-impregnated plate on the basis of UV detection.

3.3 Searching Fabry's Gb3 biomarkers

Biomarkers of Fabry disease were classified into seven groups, as reported elsewhere [5,6]: 1) six Gb_3-related isoforms with saturated fatty acyls; 2) seven methylated Gb_3-related isoforms; 3) seven Gb_3-related isoforms/analogs with one additional double bond; 4) one analog with hydrated sphingosine; 5) two Gb_3-related isoforms/analogs with two additional double bonds; 6) one short chain Gb_3-related isoform/analog; 7) one short chain methylated Gb_3-related isoform/analog.

Previous to these works, no biological methylation of ceramides in Gb_3 had been reported although the addition of methyl groups by methyltransferases is of major importance in different biological processes. The methylated-Gb_3 may be an intermediate compound in the deacylation of Gb_3 to generate the lyso-Gb_3 molecule [5].

With respect to groups 3, 5 and 6, mass spectrometry cannot differentiate between isoforms and analogs. Thus, additional double bonds can be located on fatty acyl derived chains coupled by amide linkage to the sphingosine chain in ceramide (isoforms), or in the structure of the sphingoid base, giving rise to a different base than the sphingosine.

Under our selected work conditions, Gb_3 species were found in peaks at 14.9 and 27.9 mm in the case of control plasma sample, and peaks at 14.2 and 27.7 mm in the case of Fabry's plasma, as we describe in the following sections. We did not find Gb_3-related ions in the other peaks, including that of the application area (10 mm). Other structures, probably due to LacCer and GluCer are outside the scope of this work.

Table 2 summarizes the Gb_3-related species proposed as Fabry's biomarkers in plasma by LC-MS, and those identified in this work by HPTLC-densitometry-MS, via the interface.

alt-text: Table 2-

Table 2.–

ⓘ The table layout displayed in this section is not how it will appear in the final version. The representation below is solely purposed for providing corrections to the table. To preview the actual presentation of the table, please view the Proof.

Gb_3-related species proposed as Fabry's biomarkers in plasma by LC-MS, and identified by HPTLC-MS

Fabry's biomarkers	HPTLC-ESI-MS	m/z [a] (± 1), $[M+Na]^+$	Structure number In Figure 5
Group 1: Gb_3-related isoforms with saturated fatty acyls			
d18:1;C16:0	√	1046.9	1
d18:1;C18:0	√	1074.9	2
d18:1;C20:0	X		
d18:1;C22:0	√	1130.9	3
d18:1;C24:0	√	1158.9	4
d18:1;C26:0	√	1186.9	5
Group 2: Methylated Gb_3-related isoforms			
d18:1;C16:0Me	√	1063.1	6
d18:1;C18:0Me	√	1091.1	7
d18:1;C20:0Me	√	1119.2	8
d18:1;C22:0Me	√	1146.7	9

|				
d18:1;C22:1Me		X		
d18:1;C24:0Me		√	1174.0	10
d18:1;C24:1Me		X		
	d18:1;C26:0Me [b]		1201.5	11
	d18:1;C28:0Me [b]		1229.6	12
Group 3: Gb$_3$-related isoforms/analogues with one additional double bond				
d18:1;C16:1 + d18:2;C16:0		X		
d18:1;C18:1 + d18:2;C18:0		X		
d18:1;C20:1 + d18:2;C20:0		X		
d18:1;C22:1 + d18:2;C22:0		X		
d18:1;C24:1 + d18:2;C24:0		X	1156.9*	
d18:1;C26:1 + d18:2;C26:0		X		
Group 4: Gb$_3$ analogue with hydrated sphingosine				
d18:0;C24:1 H20		X		
Group 5: Gb$_3$-related isoforms/analogues with two additional double bonds				
	d18:1;C20:2 + d18:2;C20:1 [b]		1077.4[M+H]$^+$	13
d18:1;C22:2 + d18:2;C22:1		√	1105.0[M+H]$^+$	14
d18:1;C24:2 + d18:2;C24:1		√	1132.4[M+H]$^+$	15
	d18:1;C26:2 + d18:2;C26:1 [b]		1161.0[M+H]$^+$	16
	d18:1;C28:2 + d18:2;C28:1 [b]		1188.0[M+H]$^+$	17
	d18:1;C30:2 + d18:2;C30:1 [b]		1215.0[M+H]$^+$	18
	d18:1;C32:2 + d18:2;C32:1 [b]		1243.1[M+H]$^+$	19
Group 6: Short chain Gb$_3$-related isoform/analogue				
d16:1;C16:0 + d18:1;C14:0		X		
Group 7: Short chain methylated Gb$_3$-related isoform/analogue				
d16:1;C16:0Me+ d18:1;C14:0Me		X		

[a] Ions as [M+Na]$^+$, unless otherwise stated

[b] Gb$_3$ species identified by HPTLC-MS, which were not reported as Fabry disease biomarkers but are closely related to them

X: Gb$_3$-related Fabry disease biomarkers determined by LC-MS but not by HPTLC-MS

*species not counted here as a biomarker because its corresponding ion, which accompanies the saturated Gb$_3$ d18:1; C24:0, has low intensity in the studied plasma

3.4 Saturated isoforms of Gb$_3$

Under the conditions of Figure 2, the peak at 27.7 mm (Fabry's sample) fall in the zone corresponding to migration of Gb$_3$ standard. We identified the following Gb$_3$ isoforms in this sample by HPTLC-ESI$^+$-MS and HPTLC-ESI$^+$-MS/MS, mostly as sodium adducts (with mass tolerance= ±1 *m/z*) (Figure 3): d18:1;C26:0 (*m/z* 1186.9 [M+Na]$^+$, with low intensity); d18:1;C24:0 (*m/z* 1156.9 [M+Na]$^+$), d18:1;C22:0 (*m/z* 1130.9 [M+Na]$^+$), d18:1;C18:0 (*m/z* 1074.8 [M+Na]$^+$ and *m/z* 1053.8 [M+H]$^+$), and the most preponderant form, d18:1;C16:0 (*m/z* 1046.8 [M+Na]$^+$ and *m/z* 1025.7 [M+H]$^+$). Figure 3A shows the ion profile in the HPTLC-ESI$^+$-MS spectrum with this profile, and the confirmation of identity of the most abundant ion at *m/z* 1046.8 [C$_{52}$H$_{97}$NO$_{18}$Na]$^+$, done by ESI-MS/MS. This ion was isolated and fragmented as a precursor (isolation width *m/z* 4 and amplitude voltage 1.15 V), and a product ion at *m/z* 885.2 was obtained which corresponded to the loss of a hexose [M-hexose+Na]$^+$ (Figure 3B).

alt-text: Figure 3-

Figure 3.-
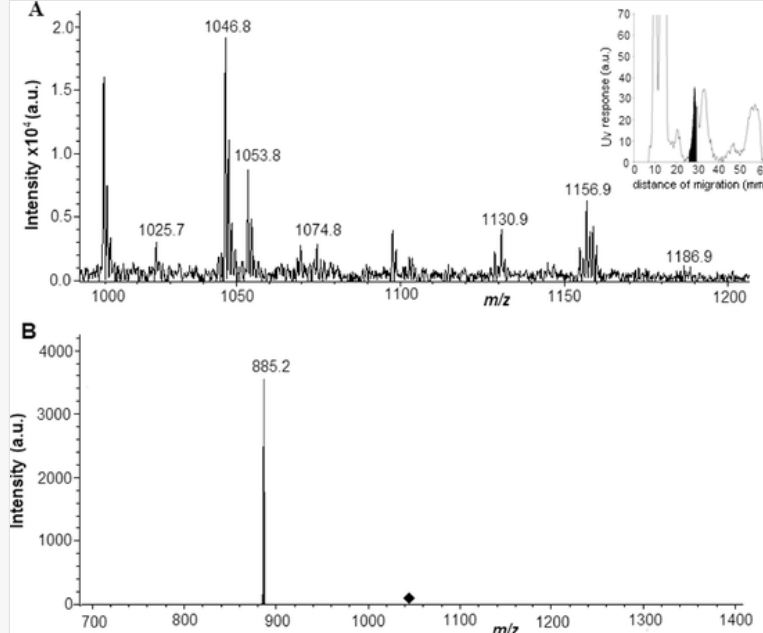
A) HPTLC-ESI$^+$-MS spectrum of peak at migration distance (m.d.) 27.7 mm (in Figure 2) from the Fabry's plasma extract, with a detail of the peak zone pierced by the interface head (in the box). The most abundant ion at *m/z* 1046 was fragmented **(B)** to obtain the HPTLC-ESI$^+$-MS/MS spectrum of this precursor ion, showing the loss of a hexose.

It has to be remarked that HPTLC-ESI$^+$-MS spectrum of healthy control sample showed Gb$_3$-related ions at much lower intensities than those of Fabry's sample. Intensities for detected ions are discussed below. Obtained signals for control sample were near LOD (Figure S1). The whole experiment for both plasma samples was performed in duplicate.

In addition to the HPTLC-ESI$^+$-MS/MS spectra, carried out on some selected ions, APCI$^+$-MS spectra was used (Figures S1B and S2) for confirming the presence of ions coming to originating from fragmentation of Gb$_3$ species to give the corresponding ceramides, as [M-3hexoses-H$_2$O+H]$^+$: *m/z* at 520.6 (d18:1;C16:0), 549.6 (d18:1;C18:0), 604.8 (d18:1;C22:0) and 632.7 (d18:1;C24:0).

3.5 Methylated-Gb3 and unsaturated Gb3 species

UV peaks at 14.9 and 14.2 mm correspond to SM class in control and Fabry's samples, respectively (Figure 2). Identified SM species were the same as reported in a previous work under other chromatographic conditions [18], and corresponded to sodium adducts of the following SM species: d18:1;C24:1 (*m/z* 835.6), d18:1;C22:0 (*m/z* 809.6), d18:1;C20:0 (*m/z* 781.6), d18:1;C18:0 (*m/z* 753.5), and d18:1;C16:0 (*m/z* 725.5) (Figure 4). Their identity was confirmed by ESI$^+$-MS/MS.

alt-text: Figure 4-

Figure 4.-
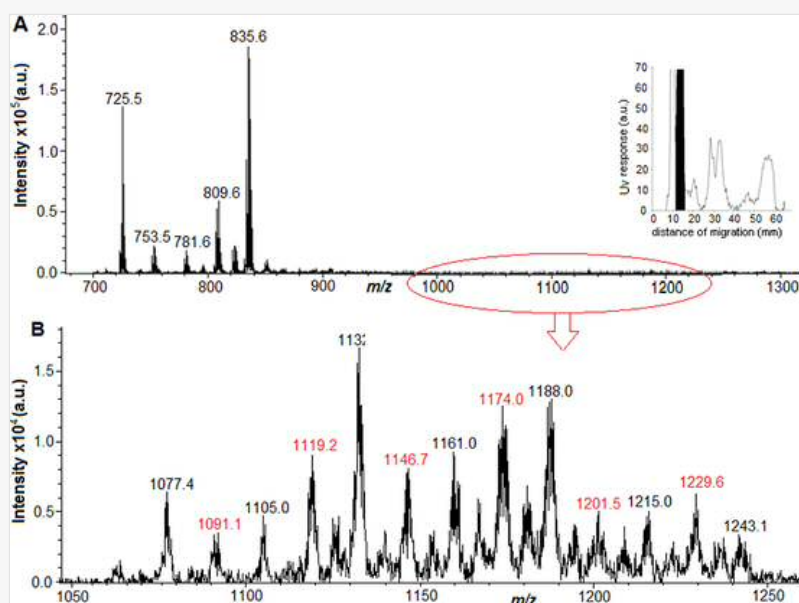
A) HPTLC-ESI$^+$-MS spectrum of peak at m.d. 14.2 mm (in Figure 2) from the Fabry's plasma extract, with a detail of the peak zone pierced by the interface head (in the box). Identified sphingomyelin (SM) species are detailed in the text. **B)** Ampliation of low-intensity ions in HPTLC-ESI$^+$-MS spectrum by window restriction to the zone of m/z >1000. Unsaturated Gb$_3$ species (black); methylated Gb$_3$ species (red). Details of ions, please see text and Table 2.

This SM peak provided a high response in UV at 190 nm. However, a residual signal at 550 nm was also found when submitted to orcinol derivatization (Figure 2). To investigate this, the SM peak was transferred from the LiChrospher plate to the ion trap-MS equipment, using the TLC-MS interface. The obtained HPTLC-ESI$^+$-MS spectra (Figure 4 in the case of Fabry's sample and Figure S3 in that of control sample) showed intensities of 10^5 arbitrary units (a.u.), and high S/N ratio for SM species. However, a slight background was perceived in the zone of m/z > 1000. Figure 4 shows a detail of this spectrum with window restriction to the zone of m/z between 1000 and 1300. This zone shows intensities of 10^4 a.u. We found that some Gb$_3$-related species are in low concentration and co-migrated together with SM species in the intense SM-peak. This experiment was performed in duplicate and similar spectra were obtained in each case. The ions found and the obtained ESI-MS profiles were similar for Fabry's plasma and control although their relative intensities were slightly different (Figures S3 and S4).

The zone between m/z 1000-1300 displays ESI ions that matched with either methylated Gb$_3$-related isoforms as [M+Na]$^+$, or Gb3-related isoforms/analogues with two additional double bonds, as [M+H]$^+$ (Table 2).

The presence of structures involving methylated-Gb$_3$ (X=CH$_3$) and Gb$_3$ with two additional double bonds (X=H) found by ESI-MS was verified by the ion fragments obtained using HPTLC-APCI, and summarized in a scheme in Figure 5. Moreover, Figure S4 displays the m/z 680-800 (A) and m/z 970-1260 (B) zones of APCI spectrum of Fabry's plasma sample. Spectra were qualitatively similar for control and Fabry's plasma.
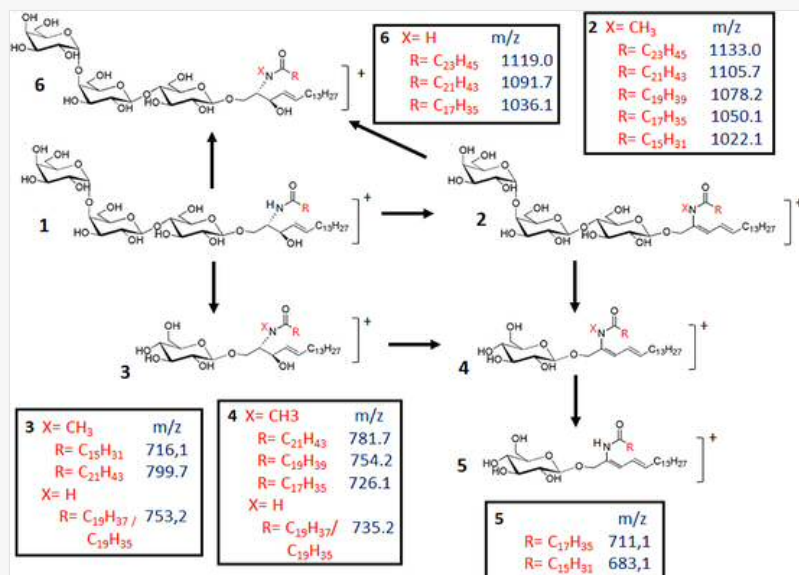
APCI-MS fragmentation for methylated Gb$_3$ (X= CH$_3$) and Gb$_3$ with two additional unsaturations (X= H).

In the m/z 970-1260 range, APCI ions were found which correspond to $[M+CH_3-H_2O+H]^+$ and $[M+H]^+$. In the m/z 680-800 range, ions corresponded to $[M+CH_3-2\text{ hexose}-H_2O+H]^+$ and $[M-2\text{ hexose}-H_2O+H]^+$.

Methylated-Gb_3 species, for example d18:1;C18:0Me, d18:1;C20:0Me, d18:1;C22:0Me, first lost a water molecule (structure 2, in Figure 5: m/z 1050.1, 1078.2, 1105.7, 1133.0, respectively), and after two hexoses (structure 4: m/z 726.1, 754.2, 781.7), respectively. Likewise, APCI fragments were found indicating that d18:1;C22:0Me also followed the route of losing both hexoses first (structure 3: m/z 799.7), and after the water molecule (structure 4: m/z 781.7).

In the case of d18:1;C16:0Me, despite of no showing an intense ESI ion at m/z 1063.1, its corresponding $[d18:1;C16:0Me-H_2O+H]^+$ ion was identified in the APCI spectrum at m/z 1022.1, as well as its derived structures 3 and 5 (Figure 5) which were identified at m/z 716.1 and 683.1, respectively. The last one corresponds to a demethylation (5) from structure 4 (Figure 5). A final demethylation was also identified in the case of d18:1;C18:0Me (m/z 711.1) after the loss of water and hexoses.

Low-intense APCI fragments were found in the cases of d18:1;C18:0Me, d18:1;C22:0Me, and d18:1;C24:0Me (m/z 1036.1, 1091.7 and 1119.0) that suggest a limited de-methylation of the N in the Gb_3 amide bond (structure 6 in Figure 5).

Gb_3 structures with two additional unsaturations refer to two ones in addition to the one present at the sphingosine base. As previously mentioned, there may be come two possibilities, either an isoform with two unsaturations in the fatty acyl chain in addition to the sphingosine base, or a different analog to sphingosine (with one more double bond) and a monounsaturated fatty acyl chain. Ions corresponding to these structures may be found in the m/z 970-1260 range of the ESI ~~APCI~~ spectrum, as $[M+H]^+$ (Figure 4): d18:1;C22:2/d18:2;C22:1 (m/z 1105.0); d18:1;C20:2/d18:2;C20:1 (m/z 1077.4); d18:1;C24:2/d18:2;C24:1 (m/z 1132.4); d18:1;C24:2/d18:2;C26:1 (m/z 1161.0); d18:1;C24:2/d18:2;C28:1 (m/z 1188.0); d18:1;C24:2/d18:2;C30:1 (m/z 1215.0); d18:1;C24:2/d18:2;C32:1 (m/z 1243.1).

However, three of these species may coexist with isobaric methylated-Gb_3 structures. Abundance of ion at m/z 1132.4 is probably due to coexistence of both $[d18:1;C24:0Me-H_2O+H]^+$ and $[d18:1;C24:2/d18:2;C24:1+H]^+$ species. Likewise, ion at m/z 1077.4 may come from both $[d18:1;C20:0Me-H_2O+H]^+$ and [d18:1;C20:2 + d18:2;C20:1]. The same for ion at m/z 1105.0 from $[d18:1;C22:0Me-H_2O+H]^+$ and [d18:1;C22:2 + d18:2;C22:1].

Almost all these species show low intensity related ions in the ESI ~~APCI~~-MS spectrum (m/z range 970-1260) that may correspond to the loss of a CH_2 group (Figure 4) (m/z at 1091.1, 1119.2, 1146.7, 1174.0, 1201.5, 1229.6). This is not shown in Figure 5. Other fragmentations for unsaturated species are depicted in Figure 5 (X=H and R corresponding to unsaturated structures). As an example, d18:1;C20:2/d18:2;C20:1 first experiences loss of two hexoses (m/z 753.0) and after, the loss of a water molecule (m/z 735.0).

As a summary, ESI and APCI ions match well with the proposed Gb3 structures.

As shown in Table 2, fourteen of the twenty-four molecular species of Gb_3 found elsewhere [5, 6] were identified using our HPTLC-MS approach. Other five new ones were also identified, which are closely structurally related to the proposed biomarkers. The HPTLC-densitometry-MS approach allowed to identify a considerable amount of Fabry biomarkers, despite the variability of plasma. In total, nineteen species of Gb_3 (Table 2) were identified by HPTLC-MS: five isoforms of saturated Gb_3; seven isoforms of methylated Gb_3 (two of which are different to those identified in [5,6]); and seven isoforms or analogs with two additional double bonds. Some isoforms/analogs with one additional double bond were detected with low intensities together the corresponding saturated isoforms although they have not been counted in our list. Comparison of Gb_3 species found using HPTLC-MS and LC-MS methods is given in Table 2 .

Intensity profiles of Gb_3 biomarkers obtained by HPTLC-densitometry-ESI$^+$-MS for Fabry's plasma sample (blue) and control (red), are depicted in Figure 6. Numbers for structures are in Table 2. Ion intensities are related to concentration of Gb_3 species for several reasons:

alt-text: Figure 6-

Figure 6.-

Figure Replacement Requested
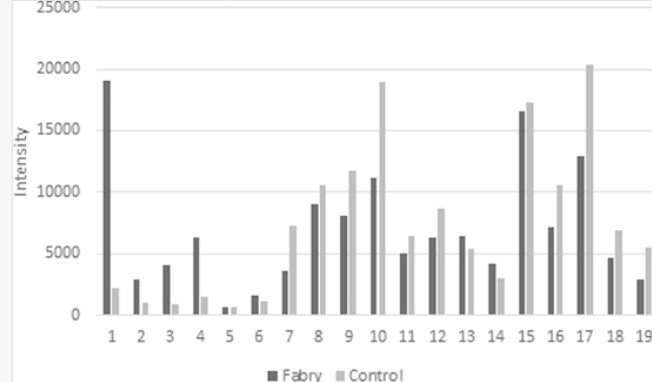
Profiles of Gb_3 species, expressed as Intensity (ion counts, arbitrary units, a.u.) for Fabry's plasma sample (blue) and control (red), obtained by HPTLC-densitometry-ESI$^+$-MS. **1-5**: Saturated Gb_3; **6-13**: methylated Gb_3; **14-19**: Gb_3 with two additional unsaturations. Structure number refers to Table 2.

Replacement Image: new fig 6 color.tif

Replacement Instruction: The previous figure was in black and grey. Now, It is the same figure but in colour. In the text and in the figure 6 caption we refer to colour. (red and blue)

- HPTLC on silica gel separates lipids in classes and, for a given class, ESI-MS responses per mass unit (response factors) are similar for the molecular species, as the influence of fatty acyl chain length is not significant[Instruction: [29] should be changed to new reference [27], as old references 24 and 25 have been deleted] [29]. Likewise, in this case, all species are structurally related, Gb_3 molecules.

- Ionization in HPTLC-MS was carried out under the same conditions for all species: AMD development solvent was removed after separation, and automated band elution was performed in all cases using MeOH. Hence, no gradients were used during ionization. In LC-based methods, the different composition of the gradient over time influences nebulization and makes response factors vary even for structurally similar lipids.

- Moreover, the interface head drills the same surface on the two extracted bands, which represents in each case an important percentage of the sample peak.

Figure 6 shows that Fabry's plasma sample is more enriched in saturated Gb_3 than the control sample and less enriched in methylated Gb_3. Regarding the species with two additional unsaturations, 13 and 14 (C20:3, C22:3) are slightly more concentrated in Fabry's but 16-19 (26:3, 28:3, 30:3, 32:3) show less concentration than the control.

4 Conclusion

The idea that HPTLC-densitometry-MS is a useful technique for identification of molecular species for Lipidomics is reinforced in this paper. In this context, the use of the interface is interesting due to the rapid, precise, and targeted characterization of selected bands. As only the zones of interest of the plate are transferred to MS, relevant information about the sample can be rapidly obtained. Thus, the positioning precision of the TLC-MS interface provided useful information about Gb_3 peak migration. HPTLC-ESI$^+$-MS spectra showed that Gb_3 ceramide tri-hexosides standard consists of an important concentration of polar hydroxyl-fatty acyls which are more retained at lower migration distance in silica gel than saturated/mono-unsaturated-Gb_3 species, causing a widening and even a splitting of the peak.

Moreover, HPTLC-MS can be perceived as a methodology to get more information online in less time from complex biological matrices. The separation on LiChrospher plates, the use of the combined densitometric techniques, and the precision of interface extraction head allowed to identify Fabry's disease biomarkers in plasma, and obtaining detailed information about the presence or absence of glyco-SL in peaks with close migration distances. Densitometric and ESI-MS profiles were repeatable and MS detection proved to be sensitive.

Saturated Gb_3 in Fabry's plasma were in higher concentration than in control sample in repeated experiments. ESI-MS profiles for methylated and unsaturated Gb_3 species were qualitatively similar for Fabry and control samples although relative distribution of ions is different.

credit author statement

Carmen Jarne: HPTLC and MS coupling experiments

Luis Membrado: Development of AMD methodology

María Savirón: mass spectrometry experiments

Jesús Vela: validation, verification and reproducibility of results/experiments and other research outputs

Jesús Orduna: design of MS strategy

Rosa Garriga: Provision of study materials, reagents, materials, analysis tools, cooperation in writing

Javier Galbán: supervisión, investigation, methodology

Vicente L. Cebolla: Preparation, creation and/or presentation of the published work, conceptualization, ideas, formulation, evolution of research goals and aims, investigation

Q2 Uncited References:

[24, 25]

Declaration of Competing Interest

We wish to confirm that there are no known conflicts of interest associated with this publication and there has been no significant financial support for this work that could have influenced its outcome.

Acknowledgements

Supplementary materials

Supplementary material associated with this article can be found, in the online version, at doi:10.1016/j.chroma.2021.461895.

References

ⓘ The corrections made in this section will be reviewed and approved by a journal production editor. The newly added/removed references and its citations will be reordered and rearranged by the production team.

[1] Touboul D., Roy S., Germain D.P., Baillet A., Brion F., Prognon P., Chaminade P., Laprevote O., Fast fingerprinting by MALDI-TOF mass spectrometry of urinary sediment glycosphingolipids in Fabry disease, Anal. Bioanal. Chem. 382 (2005) 1209–1216, doi:10.1007/s00216-005-3239-8.

[2] Ivanova M., Altered sphingolipids metabolism damaged mitochondrial functions: lessons learned from Gaucher and Fabry diseases, J. Clin. Med. 9 (2020) 1116, doi:10.3390/jcm9041116.

[3] Boutin M., Menkovic I., Martineau T., Vaillancourt-Lavigueur V., Toupin A., Auray-Blais C., Separation and analysis of lactosylceramide, galabiosylceramide, and globotriaosylceramide by LC-MS/MS in urine of Fabry disease patients, Anal. Chem. 89 (2017) 13382–13390, doi:10.1021/acs.analchem.7b03609.

[4] Aerts J.M., Groener J.E., Kuiper S., Donker-Koopman W.E., Strijland A., Ottenho R., van Roomen C., Mirzaian M., Wijburg F.A., Linthorst G.E., et al., Elevated globotriaosylsphingosine is a hallmark of Fabry disease, Proc. Natl. Acad. Sci. USA. 105 (2008) 2812–2817, doi:10.1073/pnas.0712309105.

[5] Manwaring V., Boutin M., Auray-Blais C., A Metabolomic study to identify new globotriaosylceramide-related biomarkers in the plasma of Fabry disease patients, Anal. Chem. 85 (2013) 9039–9048, doi:10.1021/ac401542k039−9048.

[6] Auray-Blais C., Boutin M., Novel Gb3 isoforms detected in urine of Fabry disease patients: a metabolomic study, Curr. Med. Chem. 19 (2012) 3241–3252, doi:10.2174/092986712800784739.

[7] Wiseman J.M., Li Jessica, Elution B., Partial separation, and identification of lipids directly from tissue slices on planar chromatography media by desorption electrospray ionization mass spectrometry, Anal. Chem. 82 (2010) 8866–8874, doi:10.1021/ac1016453.

[8] Suzuki A., Miyazaki M., Matsuda J., Yoneshige A., High-Performance Thin-Layer Chromatography/Mass Spectrometry for the analysis of neutral glycosphingolipids, Biochim. Biophys. Acta. 1811 (2011) 861–874, doi:10.1016/j.bbalip.2011.06.018.

[9] Jamin E.L., Jacques C., Jourdes L., Tabet J-C, Borotra N., Bessou-Touya S., Debrauwer L., Duplan H., Identification of lipids of the stratum corneum by High Performance Thin Layer Chromatography and Mass Spectrometry, Eur. J. Mass Spectrom. 25 (2019) 278–290, doi:10.1177/1469066718815380.

[10] Seng J.A., Ellis S.R., Hughes J.R., Maccarone A.T., Truscott R.J.W., Blanksby S.J., Mitchell T.W., Characterisation of sphingolipids in the human lens by Thin Layer Chromatography-Desorption Electrospray Ionisation Mass Spectrometry, Biochim. Biophys. Acta. 1841 (2014) 1285–1291, doi:10.1016/j.bbalip.2014.05.006.

[11] Torretta E., Fania C., Vasso M., Gelfi C., HPTLC-MALDI MS for (glyco)sphingolipid multiplexing in tissues and blood: a promising strategy for biomarker discovery and clinical applications, Electrophoresis 37 (2016) 2036–2049, doi:10.1002/elps.201600094.

[12] Jarne C., Savirón M., Lapieza M.P., Membrado L., Orduna J., Galbán J., Garriga R., Morlock G.E., Cebolla V.L., High-Performance Thin-Layer Chromatography coupled to Electrospray Ionization tandem Mass Spectrometry for identifying neutral lipids and sphingolipids in complex samples, J. AOAC Int. 101 (2018) 1993–2000, doi:10.5740/jaoacint.17-0329.

[13] Torretta E., Vasso M., Fania C., Capitanio D., Bergante S., Piccoli M., Tettamanti G., Anastasia L., Gelfi C., Application of direct HPTLC-MALDI for the qualitative and quantitative profiling of neutral and acidic glycosphingolipids: the case of NEU3 overexpressing C2C12 murine myoblasts, Electrophoresis 35 (2014) 1319–1328, doi:10.1002/elps.201300474.

[14] Bergante S., Torretta E., Creo P., Sessarego N., Papini N., Piccoli M., Fania C., Cirillo F., Conforti E., Ghiroldi A., Tringali C., Venerando B., Ibatici A., Gelfi C., Tettamanti G., Anastasia L., Gangliosides as a potential new class of stem cell markers: the case of GD1a in human bone marrow mesenchymal stem cells, J. Lipid Res. 55 (2014) 549–560, doi:10.1194/jlr.M046672.

[15] Domínguez A., Jarne C., Cebolla V.L., Galbán J., Savirón M., Orduna J., Membrado L., Lapieza M.P., Romero E., Sanz-Vicente I., de Marcos S., Garriga R., A hyphenated technique based on High-Performance Thin Layer Chromatography for determining neutral sphingolipids: a proof of concept, Chromatography. 2 (2015) 167–187, doi:10.3390/chromatography2020167.

[16] Kouzel I.U., Pirkl A., Pohlentz G., Soltwisch J., Dreisewerd K., Karch H., Muething J., Progress in detection and structural characterization of glycosphingolipids in crude lipid extracts by enzymatic phospholipid disintegration combined with Thin-Layer Chromatography immunodetection and IR-MALDI Mass Spectrometry, Anal. Chem. 86 (2014) 1215–1222, doi:10.1021/ac4035696.

[17] Schiller, J. The Simple Beauty of TLC-MALDI-MS. The analytical scientist, https://theanalyticalscientist.com/issues/1115/the-simple-beauty-of-tlc-maldi-ms/. Accessed June 2, 2020.

[18] Schiller, J.; Fuchs, B.; Suss, R.; Popkova, Y.; Griesinger, H.; Matheis, K.; Oberle, M.; Schulz, M. TLC/MALDI MS for the analysis of lipids. In: Planar Chromatography-Mass Spectrometry, Ed. by Kowalska, T.; Sajewicz, M.; Sherma. J. Chromatographic Science Series 110 (2016), 213-232. DOI: 10.1201/b19090_13.

[19] Leopold J., Popkova Y., Engel K.M., Schiller J., Recent developments of useful MALDI matrices for the Mass Spectrometric characterization of lipids, Biomolecules 8 (2018) 173–198, doi:10.3390/biom8040173.

[20] Park H., Zhou Y., Costello C.E., Direct analysis of sialylated or sulfated glycosphingolipids and other polar and neutral lipids using TLC-MS Interfaces, J. Lipid Res. 55 (2014) 773–781, doi:10.1194/jlr.D046128.

[21] https://www.matreya.com/files/fatty_acid_composition.pdf. Accessed June 2, 2020.

[22] Dreisewerd K., Müthing J., Rohlfing A., Meisen I., Vukelić Z., Peter-Katalinic J., Hillenkamp F., Berkenkamp S., Analysis of gangliosides directly from Thin-Layer Chromatography plates by infrared Matrix-Assisted Laser Desorption/Ionization orthogonal Time-of-Flight Mass Spectrometry with a glycerol matrix, Anal. Chem. 77 (2005) 4098–4107, doi:10.1021/ac048373w.

[23] Singhto N., Vinaiphat A., Thongboonkerd V., Discrimination of urinary exosomes from microvesicles by lipidomics using Thin Layer Liquid Chromatography (TLC) coupled with MALDI-TOF, Mass Spectrometry. Sci. Reports 9 (2019) 13834, doi:10.1038/s41598-019-50195-z.

[24] Gálvez E.M., Matt M., Cebolla V.L., Fernandes F., Membrado L., Cossío F.P., Garriga R., Vela J., Guermouche M.H., General contribution of nonspecific interactions to fluorescence intensity, Anal. Chem. 78 (2006) 3699–3705, doi:10.1021/ac058045b.

[25] Cebolla V.L., Mateos E., Garriga R., Jarne C., Membrado L., Cossío F.P., Gálvez E.M., Matt M., Delgado-Camón A., Changes in fluorescent emission due to non-covalent interactions as a general detection procedure for Thin-Layer Chromatography, ChemPhysChem 13 (2012) 291–299, doi:10.1002/cphc.201100590.

[Instruction: It should be the new reference [24]][26] Vasseur E., A spectrophotometric study on the orcinol reaction with carbohydrates, Acta Chem. Scandinavica. 2 (1948) 693–701, doi:10.3891/acta.chem.scand.02-0693.

[Instruction: This should be new reference 25] [27] Müthing, J. TLC and HPLC of glycosphingolipids. In carbohydrate analysis by modern chromatography and electrophoresis. El Rassi, Z. (Ed.), Journal of Chromatography Library, Vol . 66 Elsevier, The Netherlands, 2002, ch 13. DOI: 10.1016/S0301-4770(02)80038-0

[Instruction: This shloud be new reference 26] [28] Müthing J., Ziehr H., Enhanced Thin-Layer Chromatographic separation of G_{M1b}-type gangliosides by automated multiple development, J. Chromatogr. B. 687 (1996) 357, doi:10.1016/S0378-4347(96)00258-7.

[Instruction: This should be new reference 27] [29] Han X.Lipidomics, Comprehensive Mass Spectrometry of Lipids, John Wiley & Sons, Hoboken, NJ, 2016, pp. 27–28 ch. 2, doi:10.1002/9781119085263.ch1.

Highlights

- Identification of 19 Gb3 biomarkers in plasma extracts was performed by HPTLC-MS
- HPTLC-UV densitometry was coupled to MS through an automated based interface
- Saturated, methylated and unsaturated Gb3 species were identified by ESI and
- [Instruction: This is part of the previous sentence. There should be no "point"]• APCI-MS
- Saturated Gb3 species in Fabry's plasma were in higher concentration than in
- [Instruction: This is part of the previous sentence. There should be no "point"]• control
- Interface positioning precision provided information on Gb3 chromatographic

Appendix Supplementary materials

[Multimedia Component 1](#)

alt-text: Image, application 1

Queries and Answers

Q1

Query: Please confirm that givennames and surnames have been identified correctly.

Answer: Yes

Q2

Query: This section comprises references that occur in the reference list but not in the body of the text. Please position each reference in the text or, alternatively, delete it.

Answer: References 24 and 25 have been deleted. According to this, old references 26, 27, 28 and 29 should be renumbered to 24, 25, 26 and 27